Algal Research 70 (2023) 103014

Contents lists available at ScienceDirect

Algal Research

journal homepage: www.elsevier.com/locate/algal

Novel exopolysaccharide produced by the marine dinoflagellate *Heterocapsa* AC210: Production, characterization, and biological properties

Patrícia Concórdio-Reis [a,b], Martim Cardeira [c,d], Ana Catarina Macedo [c,d], Sónia S. Ferreira [e], Ana Teresa Serra [c,d], Manuel A. Coimbra [f], Ana Amorim [g], Maria A.M. Reis [a,b], Filomena Freitas [a,b,*]

[a] *Associate Laboratory i4HB – Institute for Health and Bioeconomy, School of Science and Technology, NOVA University Lisbon, Caparica, Portugal*
[b] *UCIBIO – Applied Molecular Biosciences Unit, Department of Chemistry, School of Science and Technology, NOVA University Lisbon, Caparica, Portugal*
[c] *iBET, Instituto de Biologia Experimental e Tecnológica, Apartado 12, 2781-901 Oeiras, Portugal*
[d] *Instituto de Tecnologia Química e Biológica António Xavier, Universidade Nova de Lisboa (ITQB NOVA), Av. Da Republica, 2780-157 Oeiras, Portugal*
[e] *CICECO - Department of Chemistry, University of Aveiro, Campus Universitário de Santiago, 3810-193 Aveiro, Portugal*
[f] *LAQV-REQUIMTE - Department of Chemistry, University of Aveiro, Campus Universitário de Santiago, 3810-193 Aveiro, Portugal*
[g] *MARE – Marine and Environmental Sciences Centre/ARNET - Aquatic Research Network, Faculdade de Ciências, Universidade de Lisboa, Portugal*

ARTICLE INFO

Keywords:
Marine microalgae
Dinoflagellates
Heterocapsa sp. AC210
Exopolysaccharide production
Cytotoxicity
Anti-inflammatory

ABSTRACT

Marine microalgae are promising sources of novel valuable biomolecules such as polysaccharides. In this study, the dinoflagellate *Heterocapsa* sp. AC210 was described as a new exopolysaccharide (EPS) producer. The cultivation and EPS production in bioreactor was evaluated for the first time in detail. The EPS was composed of seven different sugar monomers, including fucose and glucosamine, which are quite rare and have never been reported in dinoflagellates' EPS. Moreover, the EPS had a high content of sulphate, which is often associated with biological properties. Cytotoxicity was accessed and the results showed that the EPS did not reduce cell viability for concentrations up to 1 g L^{-1}. Additionally, antioxidant and anti-inflammatory assays demonstrated that the EPS reduced by 18 % the intracellular reactive oxygen species and decreased up to 79.3 % and 46.2 % of IL-8 and IL-6 secretion in keratinocytes, which supports its potential application in the cosmeceutical and biomedical fields.

1. Introduction

Microalgae (including cyanobacteria) are photoautotrophic microorganisms, with a key role in carbon sequestration since they convert carbon dioxide (CO_2) into organic carbon at a rate higher than organic breakdown [20,28]. In fact, microalgae account for nearly half of both CO_2 captured and O_2 produced by photosynthetic organisms annually [19].

Currently, there are several thousands of known microalgae species [20] that are present in different evolutionary lines, have contrasting ecological requirements and an enormous metabolic diversity that makes them good candidates for biodiscovery [19]. High-value biomolecules produced by microalgae include natural pigments, polyunsaturated fatty acids (PUFAs), lipids, proteins, antioxidants, vitamins, and exopolysaccharides (EPS), that are interesting to many industries, such as pharmaceutical, nutraceutical, food/feed production and skincare [3,12,20,56]. Among these different compounds, microalgae EPS are very promising, since they have been reported to have many biological properties, including anti-inflammatory, immunomodulatory, antiviral, antibacterial, antitumor and antihyperlipidaemic activities, as well as anti-coagulant and/or anti-thrombotic properties [18,30,35,52,57]. However, only recently the relevance of microalgae as producers of valuable polysaccharides has started to be considered [12]. Nevertheless, EPS producers have been identified in several microalgae, including prokaryotic cyanobacteria, within families Oscillatoriaceae, Nostocaceae and Microcoleaceae, and eukaryotic lineages, belonging to phyla Rhodophyta (Glaucosphaeraceae, Porphyridiaceae), Chlorophyta (Chlamydomonadaceae, Chlorellaceae), Charophyta (Desmidiaceae), and Bacillariophyta [20].

Within kingdom Chromista, dinoflagellates (Dinophyceae) are a

* Corresponding author at: UCIBIO-REQUIMTE, Chemistry Department, Faculty of Sciences and Technology, Universidade NOVA de Lisboa, Campus da Caparica, Caparica, Portugal.
E-mail address: a4406@fct.unl.pt (F. Freitas).

https://doi.org/10.1016/j.algal.2023.103014
Received 29 October 2022; Accepted 10 February 2023
Available online 16 February 2023

particularly interesting group due to their distinctive ecological and metabolic properties. These unicellular planktonic microalgae are found in all types of aquatic ecosystems (freshwater, marine, sea ice) and have a high trophic diversity (autotrophs, mixotrophs, heterotrophs, parasites, and symbionts) [4]. Some dinoflagellates have been reported to produce EPS with valuable properties, namely *Margalefidinium polykrikoides* (cited as *Cochlodinium polykrikoides*), that synthesized a sulphated EPS composed of mannose, galactose and glucose with antiviral activity [27]; and two *Gymnodinium* spp., both produced sulphated homopolysaccharides of galactose with immunomodulatory and antitumor activities [5,26,55,59,61]. Surprisingly, the description of dinoflagellates' EPS with biological activity is, to our knowledge, limited to the examples provided above. Given this, the exploitation of dinoflagellates as sources of EPS holds great potential to develop a strategy to capture CO_2 while producing high-value products from currently underexploited microalgae sources.

In this context, the dinoflagellate *Heterocapsa* AC210 was evaluated for the first time as an EPS producer. Microalgae growth and EPS production were investigated, and the produced EPS was characterized in terms of its chemical composition, molecular mass distribution, and thermal properties. Moreover, in vitro studies were conducted to assess the EPS cytotoxicity and biological properties, namely antioxidant and anti-inflammatory activities.

2. Materials and methods

2.1. Microorganism, pre-cultivation, and cultivation media

The microalgae used in this work, *Heterocapsa* strain AC210, originally isolated from the Balearic Sea (Spain), was obtained from the Roscoff Culture Collection (accession number RCC1514). The strain was cultured in sterile f/2 media (no added Si) (pH 8.2), with the composition described in Table 1 [24], which was prepared using natural seawater (Naturitas, Spain), after salinity adjustment (30 g L^{-1}) and sterilization (121 °C, 20 min, 2 bar). The culture was maintained at 20 °C, 16:8 h light/dark cycles, with frequent dilutions (1:2, 30 days) of the cultures in fresh f/2 medium. The inoculum was prepared by adding fresh f/2 medium (100 mL) to the microalgae cultures (100 mL) and incubation at 20 °C, with 16:8 h light/dark cycles and a light intensity of 32 μmol s^{-1} m^{-2}, provided by external fluorescent lamps (4000 K), for 7 days. The incident light intensity was measured with a LI-COR light meter (LI-250 A), equipped with a pyranometer sensor LI-200 SA (LI-COR, USA).

The photobioreactor experiments were conducted in NBP medium (NutriBloom Plus). NBP medium was prepared by supplementing natural seawater with 1 mL L^{-1} of commercial culture medium NutriBloom Plus (Necton S.A., Portugal) [21]. The final composition (after dilution) of medium NBP is presented in Table 1. This medium was chosen since it had a higher nutrient content compared to f/2 medium and could enhance microalga growth. HEPES (4-(2-hydroxyethyl)piperazin-1-ethanesulphonic acid) (20 mM) was added as pH buffer and the pH was adjusted to 8.0 by addition of NaOH (1 M).

Table 1
Composition of medium f/2 and medium NBP.

Nutrients	f/2 (mM)	NBP (mM)
Cyanocobalamin (vitamin B12)	3.69×10^{-7}	2.21×10^{-6}
Thiamine.HCl (vitamin B1)	2.96×10^{-4}	1.32×10^{-4}
Biotin (vitamin H)	2.05×10^{-6}	2.05×10^{-5}
$NaNO_3$	8.82×10^{-1}	2.00
NaH_2PO_4	3.62×10^{-2}	–
KH_2PO_4	–	1.00×10^{-1}
Na_2EDTA	1.17×10^{-2}	2.64×10^{-2}
$FeCl_3$	1.17×10^{-2}	2.00×10^{-2}
$CuSO_4$	3.93×10^{-5}	1.00×10^{-4}
$CoCl_2$	4.20×10^{-5}	1.00×10^{-4}
$MnCl_2$	9.10×10^{-4}	1.00×10^{-3}
Na_2MoO_4	2.60×10^{-5}	1.00×10^{-4}
$ZnSO_4$	7.65×10^{-5}	1.00×10^{-3}
$ZnCl_2$	–	1.00×10^{-3}
$MgSO_4$	–	2.00×10^{-3}

2.2. Photobioreactor experiments

Heterocapsa AC210 was cultivated in a cylindrical heat-sterilized 2 L bioreactor (BioStat B-plus, Sartorius, Germany) equipped with 4 sets of 30 LED lamps (4000 K) providing an incident light intensity of 98 μmol s^{-1} m^{-2} in a 16:8 h light/dark cycle. The bioreactor vessel was covered with a black acrylic structure to prevent the interference of natural light (Supplementary material, Fig. S1). Filtered air (0.2 μm) was provided at a constant flow rate of 0.4 SLPM (standard liters per minute, of compressed air) and the off gas was cooled in a condenser. The temperature was controlled at 25 °C and the stirring (70 rpm) was provided by two six blade impellers. In all experiments, the photobioreactor was inoculated with a 10 % (*v/v*) inoculum prepared as described above, with a starting OD_{750} of 0.015 ± 0.003. Culture broth samples (15 mL) were recovered daily from the photobioreactor for quantification of cell growth, nutrients' concentration, and EPS production. Each experiment was performed in at least duplicate photobioreactor runs.

2.3. Analytical techniques

Microalgae cell growth was monitored during the photobioreactor runs, by measuring the culture broth's optical density (OD) at 750 nm, using a UV–Vis spectrophotometer (CamSpec M509T), in duplicate analysis. This wavelength was previously reported for determination of cell growth for different microalgae strains without pigment interference [20,39]. For high cell concentrations (optical density higher than 1.0), samples were diluted in 0.5 M ammonium formate.

At the end of the runs, the cultivation broth was recovered from the photobioreactor and used for the gravimetric determination of the cell dry weight (CDW). Culture broth samples (240 mL) were centrifuged (11,000 ×*g*, 45 min) and the recovered cells were washed twice with ammonium formate (0.5 M) by re-suspension of the cell pellet and centrifugation (11,000 ×*g*, 45 min). The obtained pellets were freeze dried and weighted for determination of the final CDW. Triplicates were used for this analysis. The correlation between the OD_{750} and the CDW ($R^2 = 0.997$), used to estimate the CDW (g L^{-1}) of the samples withdrawn during the cultivation experiments, was determined to be as follows (Eq. (1)):

$$CDW = \frac{OD_{750} - 0.0054}{1.7002} \quad (1)$$

The samples' cell-free supernatant was used for the quantification of nitrate and phosphate and EPS production. Nitrate and phosphate concentration was determined by colorimetry using a flow segmented analyzer (Skalar 5100, Skalar Analytical, The Netherlands) [11]. EPS concentration was measured as glucose equivalent by a modified Anthrone method [15]. Anthrone (Sigma-Aldrich) solution (0.125 % in 95 % sulphuric acid, Honeywell Fluka™) was freshly prepared 2 h before use. The supernatant sample (0.5 mL) was added to a test tube containing 2.5 mL cold anthrone reagent, while the tube was kept immersed in cold water. The tubes were gently stirred to avoid heat generation and incubated for 14 min at 100 °C. After cooling on ice, the optical density was measured at 625 nm in a UV–Vis spectrophotometer. Glucose (Scharlau) solutions (5–100 mg L^{-1}) were used as standards. All analyses were performed in duplicate. Elemental analysis was performed for the EPS and the biomass, using an elemental analyzer (Thermo Finnigan-CE Instruments, Flash EA 1112 CHNS series, Italy).

2.4. Kinetic parameters calculation

The maximum specific cell growth rate μ_{max} (d^{-1}) was calculated

using the following Eq. (2):

$$ln\left(\frac{x}{x_0}\right) = \mu_{max} \times t \quad (2)$$

where x_0 is the initial biomass concentration (g L^{-1}). The overall EPS volumetric productivity (r_p, mg L^{-1} d^{-1}) and the biomass volumetric productivity (r_x, g L^{-1} d^{-1}) were determined according to Eqs. (3) and (4), respectively:

$$r_p = \frac{\Delta p}{\Delta t} \quad (3)$$

$$r_x = \frac{\Delta x}{\Delta t} \quad (4)$$

where Δp and Δx corresponds to the EPS (mg L^{-1}) and biomass (g L^{-1}) produced during the cultivation run, respectively, and Δt interval (days) corresponds to the duration of the cultivation run. The specific EPS productivity (q_p, g_{EPS} g_{CDW}^{-1} d^{-1}) was calculated using the following Eq. (5):

$$q_p = \frac{r_p}{\Delta x} \quad (5)$$

2.5. EPS extraction and purification

At the end of the cultivation runs, the culture broth was centrifuged (11,000 ×*g*, 45 min) and the supernatant was dialyzed using a 3.5 kDa MWCO (nominal molecular weight cut-off) membrane (ZelluTrans/Roth) against deionized water, at room temperature, under constant stirring. The efficiency of the process (i.e., removal of low molecular weight compounds) was monitored by measuring the conductivity of the dialysis water until it reached a value bellow 10 μS cm^{-1}. Sodium azide (10 mg L^{-1}) was added to prevent any biological contamination and possible EPS degradation. The purified EPS solution was concentrated in a rotary evaporator (Büchi Rotavapor R-210, Switzerland) operating at a pressure of 19 mbar and a temperature of 50 °C. Finally, the solution was freeze-dried and the EPS was weighted and kept in a closed vessel.

2.6. EPS physical and chemical characterization

2.6.1. EPS carbohydrate composition

The neutral sugar content of the EPS was analyzed after acid hydrolysis with 200 μL of 72 % (*w*/w) H_2SO_4 for 3 h at 25 °C, followed by 2.5 h at 100 °C in 1 M H_2SO_4 [6,49], derivatization to alditol acetates, and analysis of the individual sugars by gas chromatography with flame ionization detector (GC-FID, Perkin Elmer–Clarus 400). The GC was equipped with a 30 m column DB-225 (J&W Scientific, Fol-som, CA, USA) with internal diameter and film thickness of 0.25 mm and 0.15 μm, respectively [42]. The total sugars were obtained by the sum of the amount of the individual sugars, considering that a water molecule is added into the sugar structure when a glycosidic linkage is hydrolyzed.

Uronic acids (UA) were quantified by the colorimetric method with *m*-phenylphenol [7], using galacturonic acid (20 to 160 μg mL^{-1}) as standard in a microplate reader (Eon, BioTeK).

To identify uronic acids and amino sugars, the EPS was hydrolyzed with 2 M trifluoroacetic acid (TFA), during 1 h at 120 °C. After acid evaporation, the sample was resuspended in MilliQ water to be analyzed by high-performance anion exchange chromatography with pulsed amperometric detection (HPAEC-PAD). To identify amino sugars and uronic acids, the EPS was hydrolyzed with 2 M trifluoroacetic acid (TFA), at 120 °C, during 1 h, acid evaporated and resuspended in MilliQ water to be analyzed by high-performance anion exchange chromatography with pulsed amperometric detection (HPAEC-PAD). HPAEC-PAD analysis was performed on a Dionex ICS-6000 system consisting of DC chromatography oven and SP pump. Carbohydrates were detected by an electrochemical detector in integrated amperometry mode with AgCl reference electrode and conventional permanent gold electrode, using Chromeleon 7.3 software (Thermoscientific Dionex) and the standard carbohydrate quadruple waveform recommended for use with CarboPac columns. Separation of compounds was carried out using a Dionex CarboPac PA100 guard column (50 mm × 4 mm) and a Dionex CarboPac PA100 analytical column (250 mm × 4 mm) using gradient elution at a 1 mL min^{-1} flow rate. Eluents used were as follows: eluent A – MilliQ water, eluent B – 500 mM NaOH, eluent C – 500 mM sodium acetate. The solvents were prepared using MilliQ water (18 MΩ.cm resistance or greater); 26.4 mL of 50 % sodium hydroxide solution, MERCK, for 1 L of eluent B; 41.015 g of sodium acetate, Thermo Scientific™ Dionex™ AAA-Direct Reagents, for 1 L of eluent C, filtered through a 0.2 μm nylon filter afterwards. The eluents were used within one week. The working temperature of the column and the detector was 30 °C and initial equilibration was carried out with 0.1 % solvent B. Following manual injection of 25 μL sample onto the column, the compounds were eluted with a 55 min programme based on optimization of Dionex CarboPac PA100 Column Product Manual methods as follows: a gradient of A:B:C 99.9:0.1:0 (*v*/*v*/*v*) to 99:1:0 from 0 to 30 min; then a gradient to 50:30:20 (*v*/*v*/*v*) within 5 min, maintained for 20 min. The eluents returned to the initial ratio after the ratio of 30:30:40 for 10 min to clean impurities. Equilibration time was 30 min. To quantify the monosaccharides, calibration curves were prepared for galactose (Gal), mannose (Man), xylose (Xyl), fucose (Fuc), galactosamine (GalN), glucose (Glc), glucuronic acid (GlcA), and galacturonic acid (GalA).

2.6.2. Glycosidic linkage composition

Glycosidic linkage composition of the EPS was analyzed by methylation [44] and carboxyl reduction of methylated polysaccharides [14] to detect uronic acids linkages and improve hydrolysis of methylated polysaccharides [46]. The partially methylated alditol acetates were separated and analyzed by gas chromatography quadrupole mass spectrometry (GCqMS) (GC-2010 Plus, Shimadzu, Japan) using a non-polar column HT5 (30 m length, 0.25 mm internal diameter and 0.10 μm stationary phase, Trajan, Australia) as described by Hamed et al. [25].

2.6.3. Sulphate esters composition

Sulphate esters in the EPS were determined by turbidimetry using the barium chloride method [13,42]. The samples were submitted to a hydrolysis with 2 M TFA at 120 °C for 1 h. Then, 3.8 mL of 3 % (*w*/*v*) trichloroacetic acid and 1 mL of barium chloride-gelatin reagent (0.5 g of barium chloride in 100 mL of 0.5 % (*w*/*v*) gelatine solution) were added to 0.2 mL of the hydrolysate, which was kept at room temperature for 15–20 min. The solution was transferred to microplates and analyzed at 360 nm (Eon, BioTeK) against reagent blank containing gelatin solution instead of barium chloride-gelatin reagent. The concentration of sulphate esters was determined using K_2SO_4 as standard as SO_4^{2-} (0.05–5 mM).

To evaluate the sulphate position, the EPS were desulphated and submitted to methylation analysis, as described previously [17].

2.6.4. Pyruvate and lactate composition

Pyruvate and lactate were determined by proton nuclear magnetic resonance (^{1}H NMR) after hydrolysis of 10 mg with 1 mL of 2 M trifluoroacetic acid (TFA), at 120 °C, during 1 h, in specific speedvac tubes. After acid evaporation, the hydrolysed EPS was freeze-dried twice from 99.9 % D_2O and finally dissolved in 500 μL of 99.9 % D_2O, containing 1 % (*w*/w) of 3-(trimethylsilyl)-1-propanesulphonic acid sodium salt (DSS, Sigma-Aldrich, USA) and transferred to NMR tubes (NE-UL5–7, NEWERA, USA). ^{1}H NMR spectrum was acquired at 60 °C on Bruker 300 MHz spectrometer using zg30 sequence with 4.75 s of acquisition time and 56 number of scans. DSS was used as internal reference (22.3 μmol, 0.95 ppm) to quantify pyruvate (singlet, 2.55 ppm) and lactate (doublets, 1.55 and 1.58 ppm), according to Uhliariková et al. [54] (Fig. S2). The relative areas of ^{1}H NMR resonances were quantified using MestReNova software (Mestrelab Research S.L., Version 14.0.0-23239).

Results were expressed as dry weight percentage of EPS.

2.6.5. Fourier transform infrared spectroscopy

Fourier Transform Infra-Red (FTIR) Spectroscopy was recorded on a Perkin-Elmer Spectrum II spectrometer. The spectra were obtained between 500 and 4500 cm^{-1} after 10 scans, at room temperature.

2.6.6. Molecular mass distribution

Number and average molecular weights (Mn and Mw, respectively) of EPS, as well as the polydispersity index (Mn/Mw), were determined by Size Exclusion-High Performance Liquid Chromatography (SE-HPLC). The analysis was performed at 25 °C on a KNAUER Smartline HPLC equipped with a Phenomenex Phenogel Linear LC Column 300 × 7.8 mm (USA), using 0.1 M $LiNO_3$ as eluent, at a flow rate of 0.6 mL min^{-1}. 50 μL of EPS solution (0.5 *w/v*% in 0.1 M $LiNO_3$) were injected and a Water 2414 Refractive Index Detector (RID) was used for detection. The values of Mw and Mn were calculated using a calibration curve generated with pullulan standards (P50 to P80)[45].

2.6.7. Thermogravimetry (TG) analysis

EPS samples (~10 mg) were characterized by Thermogravimetry (TG) using a Thermogravimetric Analyzer Labsys EVO (Setaram, France), with a heating rate of 10 °C min^{-1}, from 25 to 500 °C. The thermal degradation temperature (T_{deg}, °C) corresponds to the temperature value obtained for the maximum decreasing peak of the sample mass.

2.6.8. Elemental analysis

The elemental analysis of the EPS was performed using an elemental analyzer (Thermo Finnigan-CE Instruments, Flash EA 1112 CHNS series, Italy). The samples are subjected to a flash combustion in an oxygen environment and the resulting gases (N_2, CO_2, H_2O and SO_2) are separated by gas chromatography. Finally, the content of nitrogen, carbon, hydrogen, and sulphur was calculated using a thermal conductivity detector.

2.7. Biological assays

2.7.1. Cell culture

Biological assays were performed using the human immortalized keratinocyte cell line HaCaT, obtained from Deutsches Krebsforschungszentrum (DFKZ, Germany), and the human fibroblast cell line CCD-1079Sk obtained from American Type Culture Collection (ATCC, USA). HaCaT cells were cultured in Dulbecco's Modified Eagle medium (DMEM) supplemented with 10 % (*v/v*) of heat-inactivated fetal bovine serum (FBS) and 1 % (*v/v*) penincilin-strepmycin (PS). CCD-1079Sk cells were cultured in DMEM medium supplemented with 10 % (*v/v*) FBS and 1 % (*v/v*) non-essential amino acids (NEAA). Cells were maintained at 37 °C with 5 % CO_2, as described by Concórdio-Reis et al. [10].

2.7.2. Cytotoxicity assays

The HaCaT and CCD-1079Sk cells were seeded into 96-well plates at a density of 4.5 × 10^5 cells mL^{-1} and 1.5 × 10^5 cells mL^{-1} and allowed to grow for 72 and 24 h, respectively. At the day of the assay, cells were incubated with the EPS diluted in culture medium supplemented with 0.5 % FBS and 1 % PS at concentrations of 62.5 μg mL^{-1}; 125 μg mL^{-1}; 250 μg mL^{-1}; 500 μg.$mL^{-1}$and 1000 μg mL^{-1}. Cells incubated only with culture medium were considered as control. After 24 h, cells were washed once with PBS (Sigma-Aldrich, USA) and cell viability was assessed using CellTiter 96® AQueous One Solution Cell Proliferation Assay (Promega, USA) containing MTS reagent, according to manufacturer's instructions. The optical density was measured at 490 nm using a BioTek EPOCH2 Microplate Reader (BioTek, USA) and cell viability was expressed in terms of percentage of living cells relative to the control. A minimum of three independent experiments were performed in triplicate.

2.7.3. Cellular antioxidant activity

Cellular antioxidant activity was evaluated following previously described methods [38,50], with some modifications. Briefly, HaCaT cells were seeded at a density of 1.4 × 10^5 cells cm^{-2} in 96 well plates and the formation of intracellular reactive oxygen species (ROS) was monitored using 2′,7′-dichlorofluorescein diacetate (DCFH-DA) as a fluorescent probe. 72 h after seeding, cells were washed with PBS and treated with selected non-toxic concentrations (62.5 μg mL^{-1}; 125 μg mL^{-1}; 250 μg mL^{-1}; 500 μg mL^{-1}; 1000 μg mL^{-1}) of the samples and 25 μM DCFH-DA in PBS for 1 h. Subsequently, cells were washed again with PBS and incubated with the stress inducer (600 μM AAPH in PBS) for 1 h. After that, fluorescence was measured in a FL800 microplate fluorescence reader (Bio-Tek Instruments, Winooski, VT, USA) (Ex/Em 485 ± 20/528 ± 20 nm). The results were expressed as ROS percentage relative to the untreated control (cells treated with DCFH-DA and AAPH). Three independent experiments were performed in triplicate.

2.7.4. Anti-inflammatory activity

HaCaT cells were seeded at a density of 1 × 10^5 cell cm^{-2} in 12 well plates. After 3 days, cells were stimulated with 15 μg mL^{-1} of lipopolysaccharides (LPS) from *Escherichia coli* and co-incubated with different concentrations of each sample (62.5; 125; 250; 500; 1000 μg mL^{-1}) diluted in culture medium (DMEM medium containing 0.5 % FBS). Cells incubated only with LPS in culture media and with only culture media were used as positive and negative control, respectively. After 24 h, supernatants were collected, centrifuged for 10 min at 2000 *xg* and stored at −80 °C until further analysis. Interleukin-8 (IL-8) level was assessed by enzyme-linked immunosorbent assay (ELISA), using commercially available kits (PeproTech; London, UK), according to the manufacturer's instructions, with absorbance measured at 450 nm with wavelength correction set at 620 nm in a microplate spectrophotometer (EPOCH 2, BioTek Instruments).

3. Results and discussion

3.1. Microalgae growth and EPS production

Heterocapsa AC210 cell growth and EPS production on NBP medium was evaluated (Fig. 1), and the kinetic parameters obtained in the bioreactor cultivation were determined (Table 2). After a short adaptation period (first day), *Heterocapsa* AC210 grew exponentially for 5 days before entering a stationary growth phase (Fig. 1), reaching a maximum cell dry weight of 0.38 ± 0.01 g L^{-1} at the end of the cultivation run (8 days). A maximum specific growth rate (μ_{max}) of 0.464 ± 0.133 d^{-1} was attained between days 2 and 5 (Table 2). This value is

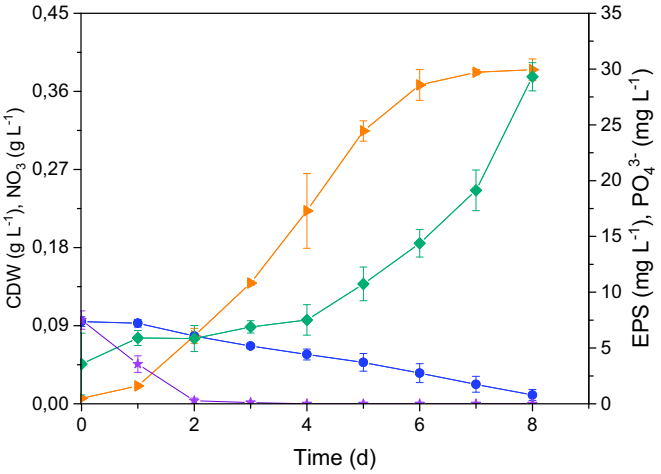

Fig. 1. Cultivation profile (CDW (▸), EPS (◆), nitrate concentration (●) and phosphate concentration (★)) of *Heterocapsa* AC210 grown on NBP medium.

Table 2
Kinetic parameters (μ_{max}, maximum specific growth rate; r_p, EPS volumetric productivity; r_x, biomass volumetric productivity; q_p, EPS specific productivity) obtained in the bioreactor cultivation experiment.

Parameters	
CDW (g L^{-1})	0.38 ± 0.01
EPS (mg L^{-1})	25.7 ± 3.0
μ_{max} (d^{-1})	0.464 ± 0.133
r_p (mg_p L^{-1} d^{-1})	3.22 ± 0.38
r_x (g_x L^{-1} d^{-1})	0.047 ± 0.002
q_p (mg_p g_x^{-1} d^{-1})	8.50 ± 1.04

within those reported for the dinoflagellate *Gymnodinium impudicum* strain KG03 (0.435–0.688 d^{-1}) [60].

Concomitant with cell growth, nutrient consumption was observed with phosphate and nitrate being completely consumed within 2 and 8 days of cultivation, respectively (Fig. 1). Phosphate depletion strongly affects microalgae cell generation, thus, affecting cell growth [39]. Nitrogen has an essential role for cell proliferation and protein synthesis in microalgae [39]. In some species, low nitrate concentrations favor the shift to the stationary phase and induce EPS production as a response to starvation [12,39]. This seemed to be the case for *Heterocapsa* AC210, since EPS production was initiated during exponential cell growth and increased concomitant with microalgae growth and nitrogen consumption (Fig. 1). When the culture reached the stationary cell growth phase, significant EPS production was observed, suggesting that the production of EPS is partially growth associated. At the end of the cultivation run, a maximum EPS concentration of 25.7 ± 3.0 mg L^{-1} was reached, resulting in an overall EPS volumetric productivity (r_p) of 3.22 ± 0.38 mg_p L^{-1} d^{-1} (Table 2). Similar results were reported for dinoflagellate *G. impudicum* strain KG03, where EPS production was growth associated. The EPS concentration was found to be between 17.5 mg L^{-1} (standard cultivation conditions) and 134.7 mg L^{-1} (optimized cultivation conditions), and the r_p values were in the range of 0.92–7.09 mg_p L^{-1} d^{-1} [60].

3.2. EPS characterization

3.2.1. Physicochemical composition

The EPS from microalgae *Heterocapsa* AC210 had a heterogeneous composition, comprising neutral sugars, namely galactose (Gal, 20 mol %), mannose (Man, 16 mol%), xylose (Xyl, 14 mol%), fucose (Fuc, 9 mol %), galactosamine (GalN, 7 mol%), and glucose (Glc, 6 mol%); and uronic acids, namely, glucuronic acid (GlcA, 22 mol%) and galacturonic acid (GalA, 6 mol%). Lactate (0.34 mg g^{-1}) and pyruvate (0.14 mg g^{-1}) were found as substituents (Table 3, Fig. S2). Although few examples are known, dinoflagellates were reported to synthesize galactose-rich EPS [47,61]. A similar composition was found for the EPS produced by *Gymnodinium* A_3 OKU-1 strain, an EPS composed of galactose and sulphate in similar proportions [26]. Lactate was also detected in its composition [26]. On the other hand, the toxic dinoflagellate *Amphidinium carterae* secreted an EPS composed of Gal (73 mol%) and Glc (27 mol%) residues [37]; whereas the EPS from *M. polykrikoides* was mainly composed of Man, Gal, Glc and uronic acids [27]. Thus, to the best of our knowledge, our results report, for the first time, the presence of Fuc, Xyl and GlcN in dinoflagellates' EPS.

Moreover, the EPS had a high content of sulphate (29.7 ± 2.8 wt%). The high content of sulphate may indicate that the salts were not completely removed from the polysaccharides. As the mol% ratio of sulphate to the carbohydrate residues is 3.6, it shows that not all the sulphate is linked to the polysaccharide. Nevertheless, the presence of sulphate substituents is a common feature of dinoflagellate exopolysaccharides. In fact, the EPS produced by marine dinoflagellates such as *Gyrodinium impudicum* KG03 and *M. polykrikoides*, were found to comprise sulphate groups with contents of 10.3 and 7–8 wt%, respectively [27,61]. Moreover, sulphate was also detected in the EPS produced by two *Lepidodinium chlorophorum* strains [47]. Additionally, elemental analysis showed a low content in nitrogen (0.62 wt%), which indicated that the EPS did not have a high protein content.

3.2.2. Glycosidic linkages

The EPS produced by *Heterocapsa* AC210 had a wide range of glycosidic linkages of Fuc, Xyl, Man, Gal, and Glc, as well as (1 → 3,4)-Glc*p*A and t-Gal*p*A, determined by a non-quantitative carboxyl reduction (Table 3). Fuc was found as *t*-Fuc*p* (0.8 mol%) or (1 → 4)-Fuc*p* (1.3 mol %) with substituents or ramifications at position 2 and 3 (4.1 and 2.8 mol%, respectively). Xyl was found as *t*-Xyl*p* (5.6 mol%), (1 → 2)-Xyl*p* (1.0 mol%), (1 → 4)-Xyl*p* (5.8 mol%), and (1 → 2,4)-Xyl*p* (1.6 mol%). Gal was mainly found as *t*-Gal*p* (5.6 mol%), followed by (1 → 6)-Gal*p* (3.5 mol%), (1 → 2)-Gal*p* (2.5 mol%), and (1 → 4)-Gal*p* (2.5 mol%), which were also substituted at positions 2 or 3 (2.4 mol% of (1 → 2,3)-Gal*p;* 1.9 % of (1 → 3,6)-Gal*p*; 0.9 % of (1 → 2,6)-Gal*p*; and 0.7 % of (1 → 3,4)-Gal*p*). Glc was mainly observed as (1 → 4)-Glc*p* (3.0 %). *t*-Glc*p* (0.6 mol%), (1 → 2,4)-Glc*p* (0.6 mol%), (1 → 3,6)-Glc*p* (0.4 mol%), (1 → 2,3,6)-Glc*p* (0.7 mol%), and (1 → 3,4,6)-Glc*p* (0.7 mol%) were also found. Although highly substituted, the content of linkages is not enough to explain the high content of sulphate determined in the

Table 3
Sugar composition (mol%) of *Heterocapsa* AC210 EPS and glycosidic linkage before and after desulphation.

	Sugar composition (mol%)								Substituents composition (mg g^{-1})		
	Fuc	Xyl	Man	Gal	Glc	GalA	GlcA	GalN	Sulph	Pyr	Lac
EPS composition	9	14	16	20	6	6	22	7	297	0.14	0.34
Glycosidic linkages											
t-Linked	0.8 (0.6)	5.6 (4.5)	11.2 (14.9)	5.6 (4.9)	0.6 (0.7)	nd	✓	nd			
(1 → 2)-linked	nd	1.0 (1.3)	nd	2.5 (3.0)	nd	nd	nd	nd			
(1 → 4)-linked	1.3 (3.2)	5.8 (7.5)	2.1 (1.1)	2.5 (3.4)	3.0 (4.2)	nd	nd	nd			
(1 → 6)-linked	nd	nd	nd	3.5 (4.3)	nd	nd	nd	nd			
(1 → 2,3)-linked	nd	nd	nd	2.4 (2.6)	nd	nd	nd	nd			
(1 → 2,4)-linked	4.1 (4.3)	1.6 (0.7)	nd	nd	0.6 (0.1)	nd	nd	nd			
(1 → 2,6)-linked	nd	nd	nd	0.9 (1.2)	nd	nd	nd	nd			
(1 → 3,4)-linked	2.8 (0.9)	nd	2.7 (tr)	0.7 (0.6)	nd	✓	nd	nd			
(1 → 3,6)-linked	nd	nd	nd	1.9 (tr)	0.4 (0.3)	nd	nd	nd			
(1 → 2,3,6)-linked	nd	nd	nd	nd	0.7 (0.3)	nd	nd	nd			
(1 → 3,4,6)-linked	nd	nd	nd	nd	0.7 (0.4)	nd	nd	nd			

Values in brackets are from glycosidic linkage composition after desulphation nd – not detected; tr – traces; Sulphate – Sulph; Pyr – pyruvate; Lac – lactate.

sample, showing the presence of salts.

To evaluate the sulphate esters positions and composition, the EPS was desulphated before glycosidic linkage analysis. The desulphation distinguishes if the substitution of a sugar residue is a branching point or a sulphate ester. When a substitution remains after desulphation, it indicates that this position contains a branching point. On the other hand, the decrease of substituted linkages indicates the presence of sulphate esters at those positions. After desulphation, an increase of (1 → 4)-Fuc*p* occurred with a decrease of (1 → 3,4)-Fuc*p*, indicating that 21 % of Fuc residues were substituted at position 3 (Table 3). Desulphated EPS had an increase of (1 → 4)-Xyl*p* occurred with a decrease of (1 → 2,4)-Xyl*p*, indicating that 6 % of Xyl residues were substituted at position 2. An increase of 23 % of t-Man*p* residues occurred with a concomitant decrease of (1 → 4)-Man*p* and (1 → 3,4)-Man*p*, indicating the presence of Man mainly as t-Man*p* (93 % of total Man) with sulphate esters at position 4 or at positions 3 and 4. Increase of (1 → 4)-Gal*p* and (1 → 6)-Gal*p* with decrease of (1 → 3,4)-Gal*p* and (1 → 3,6)-Gal*p*, indicates the presence of 10 % of Gal with sulphate esters at position 3. Decrease of (1 → 2,4)-Glc*p*, (1 → 3,6)-Glc*p*, (1 → 2,3,6)-Glc*p*, (1 → 3,4,6)-Glc*p* residues occurred with increase of (1 → 4)-Glc*p*, indicating the presence of 22 % Glc substituted sulphate esters at position 2 and/or positions 3 and 6.

3.2.3. FTIR analysis

The FTIR spectrum of the EPS produced by *Heterocapsa* AC210 (Fig. 2) showed an intense broad band at around 3000–3500 cm^{-1} with a peak at 3334 cm^{-1} that corresponds to the stretching vibration of hydroxyl groups [9,16,61]. This band partially overlaps the C—H stretching peak of CH_2 groups (2924 cm^{-1}), and the band at around 3250 cm^{-1} characteristic of the N—H stretching vibration [9,16,51]. The peaks at 1646 cm^{-1} and 1414 cm^{-1} are characteristic of the C═O asymmetric and symmetric stretching vibrations, respectively [9,61]. The absorption region at around 1230 cm^{-1} can be attributed to the stretching vibration of S═O from sulphate groups and/or of C-O-C from acyl substituents [9,43,61]. The peak at 1078 cm^{-1} can be assigned to C—O and C—C vibrations of the glycosidic bonds and pyranose ring [9], and/or the vibration of S═O and C-O-S groups [37]. Finally, the peak at around 600 cm^{-1} could also result from the glycosidic linkage bond [37].

3.2.4. Molecular mass distribution

The molecular mass distribution analysis of *Heterocapsa* AC210 EPS revealed two distinct chromatographic peaks, suggesting that the sample comprised two high molecular weight saccharide fractions, with $7.55 \pm 0.97 \times 10^5$ and $4.50 \pm 0.73 \times 10^4$ Da, and polydispersity index (PDI) of 1.51 ± 0.01 and 1.22 ± 0.06, respectively. Similarly, the EPS synthesized by the dinoflagellates *A. carterae* and *M. polykrikoides* were composed of two polysaccharide fractions with Mw values of 2.2×10^5 and 1.3×10^3 Da, and of 1.3×10^6 and 6.3×10^5 Da, respectively [27,37]. In contrast, the EPS produced by *G. impudicum* KG03 and *Gymnodinium A3 OKU-1* presented only one polysaccharide fraction, with Mw values of 1.87×10^6 and 1.3×10^6, respectively [26,61].

3.2.5. Thermal properties

The TGA curve of *Heterocapsa* AC210 EPS displayed two main degradation steps (TGA data in Supplementary Material, Fig. S3). An initial weight loss of 21 % is observed between 37 and 194 °C due to moisture loss [9,37,61]. High moisture content has previously been described for dinoflagellates' EPS and might be due to the high affinity of water molecules to carboxyl groups present in the polysaccharide [37,61]. Above this temperature, a second weight loss of 21 % occurred, corresponding to the decomposition of the polysaccharide chains, in accordance with sugar analysis. The EPS thermal degradation (T_{deg}) was found to be 239 °C, a value similar to that reported for the EPS produced by the dinoflagellate *G. impudicum* KG03 (250 °C) [61] and within the range of values reported for other microbial EPS (111–300 °C) [1,9,31,43]. The EPS showed a high char yield (54.6 %) that could be due to the high sulphate content, a complex molecular configuration and the presence cations that might bind to the different charged sugar moieties [9,43].

3.3. Biological assays

3.3.1. Cytotoxicity assessment

The potential cytotoxicity of the *Heterocapsa* sp. AC210 EPS was evaluated in both human keratinocytes (HaCaT) and human fibroblasts (CCD-1079Sk), which are the predominant cell types found in skin, representing the epidermal and dermal layers, respectively [38]. These cell lines play a major role in the biological response for maintaining skin integrity [10,38] and are among the cell lines recommended by ISO 10993-5 international standard for cytotoxicity assessment. As shown in Fig. 3, the EPS did not induce any cytotoxic effect to the cell lines tested since cell viability was not affected in the presence of EPS concentrations

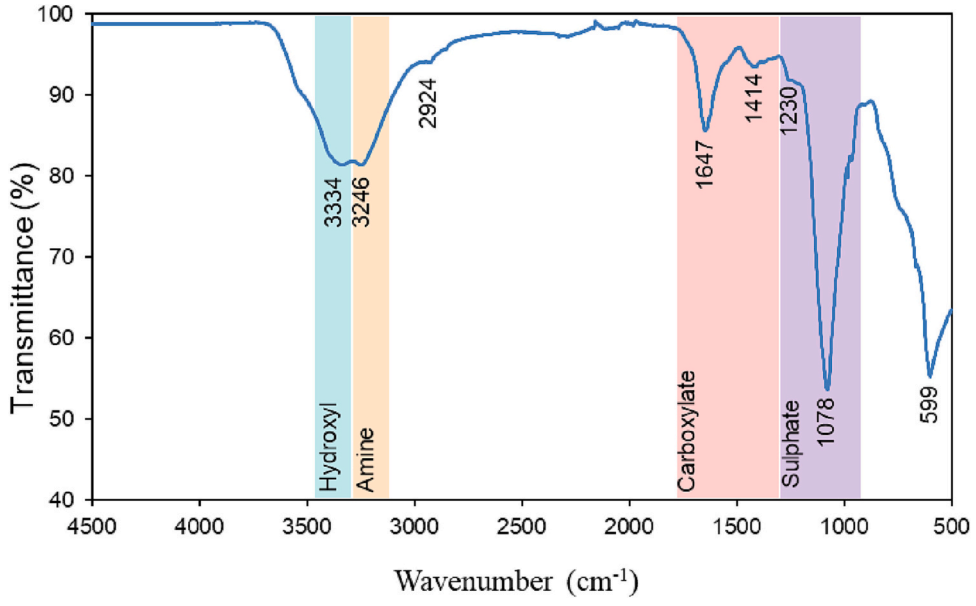

Fig. 2. FTIR spectrum of the EPS produced by *Heterocapsa* AC210.

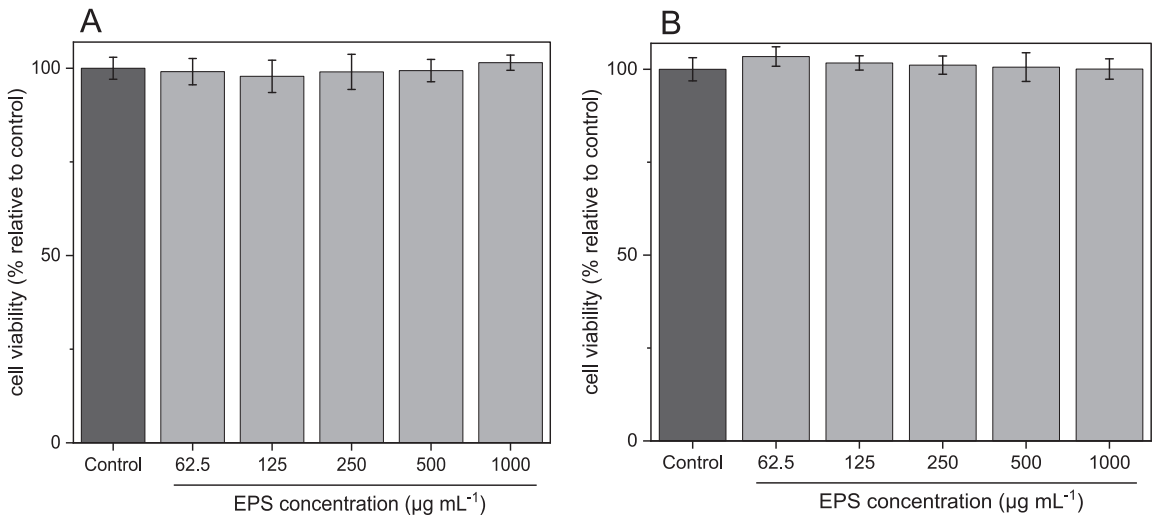

Fig. 3. Effect of *Heterocapsa* AC210 EPS on the viability of HaCaT (A) and CCD-1079Sk cell lines after 24 h incubation. Results were expressed in terms of mean ± SD of three independent experiments performed in triplicates.

up to 1000 μg mL^{-1}. These results are consistent with literature, as the biocompatibility of several polysaccharides such as alginate, hyaluronic acid and xanthan gum were demonstrated for the same polymer concentration range [22,41].

3.3.2. Cellular antioxidant activity

The capacity of *Heterocapsa* sp. AC210 EPS to inhibit ROS production in HaCaT cells was evaluated for polymer concentrations between 62.5 and 1000 μg mL^{-1} (Fig. 4). Compared to the control, a decrease of the ROS production was observed concomitant with an increasing EPS concentration, indicating that the EPS has antioxidant properties. In the presence of only 250 μg mL^{-1} of EPS, ROS production decreased by 14.3 %. At the maximum concentration tested (1000 μg mL^{-1}), a 18.3 % reduction in the ROS level was observed. Similarly, several natural polysaccharides from different sources have been reported to reduce ROS production in a variety of cell lines after exposure to different oxidative agents. Examples include the plant polysaccharide (*Sophora subprosrate*) that, at concentrations between 100 and 400 μg mL^{-1}, significantly decreased the ROS level in mouse macrophage cell line (RAW264.7 cells) infected with porcine circovirus type 2 (PCV2) [53]. The polysaccharide extracted from *Cyclocarya paliurus* plant reduced ROS production in H_2O_2-induced RAW264.7 cells in a dose-dependent manner from 25 to 100 μg mL^{-1} [58]. Additionally, the sulphated-polysaccharide extracted from the seaweed *Sargassum thunbergia*, at concentrations between 25 and 100 μg mL^{-1}, reduced H_2O_2-induced ROS production (~30 to ~40 %) in African green monkey kidney (Vero) cells [32]. Also, treatment with different concentrations of arabinan-rich pectic polysaccharide from acerola (25–200 μg mL^{-1}), ROS concentration in H_2O_2-induced NIH 3 T3 murine fibroblast cells decreased significantly [33]. In the presence of the microalgae *Porphyridium* sp. Polysaccharide, ROS level in human coronary artery endothelial cells (HCAECs) decreased by ~30 % [34]. After only 1 h of treatment with the fucose-rich exopolysaccharide produced by *Bacillus megaterium* RB-05 (200 and 250 μg mL^{-1}), a significant reduction of ROS levels was observed in H_2O_2-induced human lung fibroblasts cells (WI38) [48].

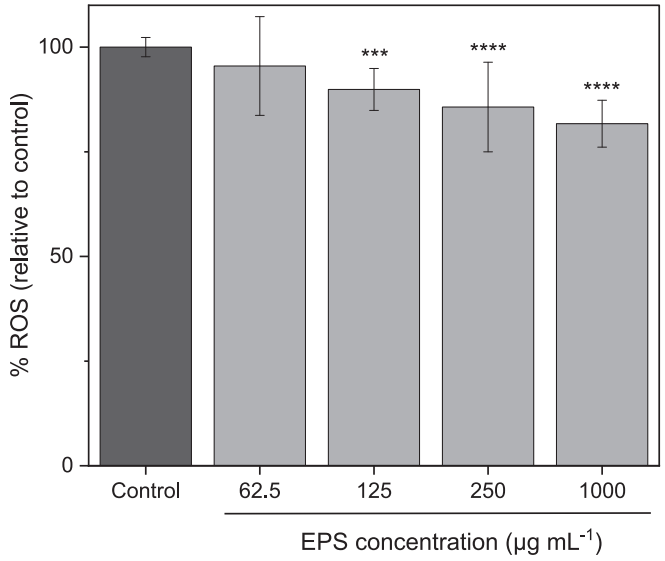

Fig. 4. Effect of *Heterocapsa* AC210 EPS on the inhibition of AAPH-induced ROS production in HaCaT cells. The results were expressed as ROS percentage relative to the untreated control (cells treated with AAPH), in terms of mean ± SD of three independent experiments. Statistically significant differences between the samples and the control were calculated according to *t*-test (*** $p \leq 0.001$, **** $p \leq 0.0001$).

Free radicals such as reactive oxygen species (ROS) can cause oxidative stress in essential cellular structures (e.g., lipids, DNA, proteins) of living organisms, leading to altered functionality [19,38]. Even though ROS overproduction might occur due to environmental factors, cellular exposure to ROS is inevitable as these species are formed as a consequence of aerobic metabolism [23,38]. These oxidant species contribute to the skin ageing process, either directly by causing damages in the biomolecules, or indirectly by interfering with the signaling pathways of keratinocytes and fibroblasts [38]. Moreover, ROS can severely affect the skin wound healing capacity, as they cause cell death, less flexibility of skin lipids, and proteases inhibitors oxidative damage [36].

3.3.3. Anti-inflammatory activity

The anti-inflammatory activity of the EPS produced by *Heterocapsa* sp. AC210 was evaluated as the capacity to reduce the release of inflammatory cytokine IL-8 (Fig. 5 A) and IL-6 (Fig. 5 B) by HaCaT cells after an inflammatory stimulus induced by LPS. As Fig. 5 A shows, *Heterocapsa* sp. AC210 EPS presented an anti-inflammatory effect for all concentrations tested, with the IL-8 secretion reducing up to 79.3 %. Interestingly, for concentrations higher than 500 μg mL^{-1}, *Heterocapsa* sp. AC210 EPS efficiency in reducing IL-8 secretion was comparable to that of IKK-2 and IKK-1 inhibitor BMS (5 μM), a commercial anti-inflammatory substance (no statistical difference for a 95 %

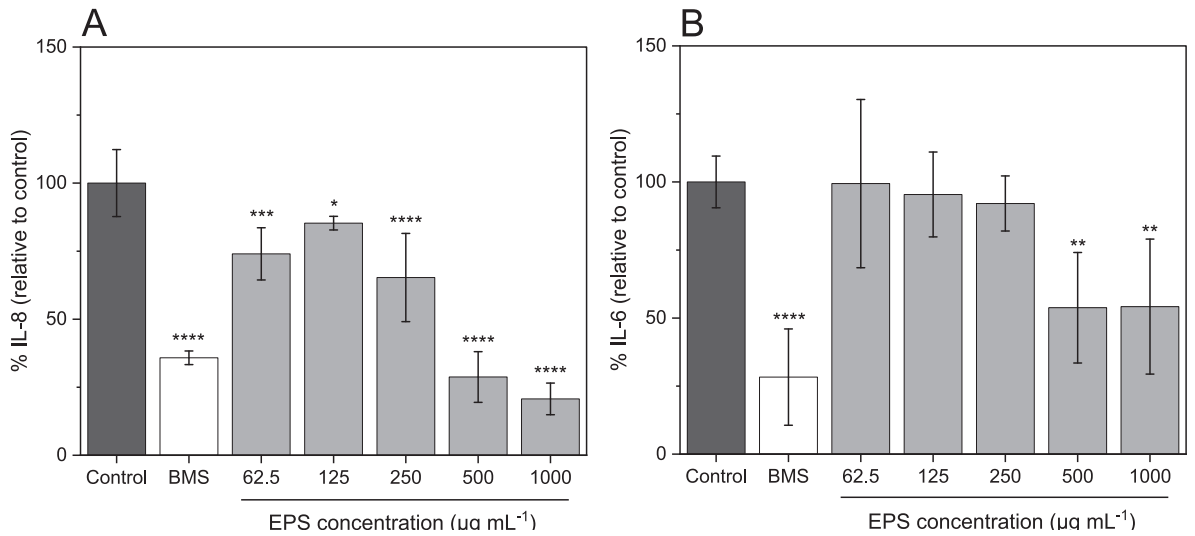

Fig. 5. Effect of *Heterocapsa* AC210 EPS on the IL-8 (A) and IL-6 (B) cytokine secretion in HaCaT cells challenged by LPS. BMS (5 µM) was used as a comparative commercially available anti-inflammatory agent. Results were expressed in terms of mean ± SD of three independent experiments. Statistically significant differences between the samples and the control were calculated according to *t*-test (** $p \leq 0.01$, *** $p \leq 0.001$, **** $p \leq 0.0001$).

confidence level). Additionally, IL-6 levels decreased 46.2 % for EPS concentrations above 500 µg mL^{-1} ($p \leq 0.01$) (Fig. 5 B).

The biological properties of the polysaccharides, including their anti-inflammatory activity, seem to be related to the complex interaction of several factors such as their structure, composition, sulphation level, distribution of sulphate groups along the backbone of the polysaccharide, molecular weight, and stereochemistry [8]. Therefore, contradictory results have been reported in literature. For instance, the heteroglycan isolated from cyanobacteria *Nostoc commune* significantly reduced secretion of IL-6 in LPS-stimulated human monocytes at concentrations above 10 µg mL^{-1}. On the contrary, it increased the production of pro-inflammatory cytokine IL-8, being more than three-fold at the highest concentration tested (100 µg mL^{-1}) [40]. The sulphated polysaccharide from *Sargassum swartzii* (34 % sulphate) exhibited anti-inflammatory activity by reducing IL-6 production in LPS-induced macrophages (RAW 264.7) for concentrations above 50 µg mL^{-1} ($p \leq 0.05$) [29]. Also, in monocytes challenged with LPS, heparin resulted in an increase of IL-6 production, whereas dextran and fucan (sulphate content of 29 %) did not affect the production of this cytokine [2]. In this study, only the semisynthetic dextran derivatives (DD) randomly substituted with carboxymethyl, benzylamide, sulphonate, and sulphate groups (21 %), resulted in a decrease of 20–30 % in IL-6 production [2]. As for IL-8 production, an inhibition of 61 and 65 % was observed in the presence of heparin and DD, respectively [2]. These results suggest that *Heterocapsa* AC210 EPS had significant anti-inflammatory activity by reducing pro-inflammatory cytokines production. Such bioactive compound might be useful in the treatment of chronic wounds [30] or skin inflammatory diseases such as atopic dermatitis or psoriasis [8].

4. Conclusions

The dinoflagellate microalgae *Heterocapsa* sp. AC210 was investigated as an EPS producer. Monosaccharide analysis revealed the presence of seven different sugar monomers, including fucose, xylose and glucosamine, which have never been reported in dinoflagellates' EPS before. Additionally, the EPS had a high content of sulphate, which is associated with the biological properties often found for microalgae' EPS. Up to 1000 µg mL^{-1} the EPS was not cytotoxic and in vitro bioactivity tests revealed its antioxidant and anti-inflammatory activities. These findings establish a valuable starting point for both the production of this high value EPS, and the development of new EPS-based bioactive materials with potential application in the cosmeceuticals and biomedicine fields. Nonetheless, EPS production should be optimized in the future for commercial development.

CRediT authorship contribution statement

Patrícia Concórdio-Reis: Conceptualization, Methodology, Investigation, Formal analysis, Writing – original draft. **Martim Cardeira:** Methodology, Investigation, Formal analysis. **Ana Catarina Macedo:** Methodology, Investigation, Formal analysis. **Sónia S. Ferreira:** Methodology, Investigation, Formal analysis. **Ana Teresa Serra:** Formal analysis, Writing – review & editing. **Manuel A. Coimbra:** Formal analysis, Supervision, Writing – review & editing. **Ana Amorim:** Funding acquisition, Supervision, Writing – review & editing. **Maria A. M. Reis:** Funding acquisition, Supervision, Writing – review & editing. **Filomena Freitas:** Conceptualization, Funding acquisition, Supervision, Writing – review & editing.

Declaration of competing interest

The authors declare that they have no known competing financial interests or personal relationships that could have appeared to influence the work reported in this paper.

Data availability

Data will be made available on request.

Acknowledgments

This work was supported by Research Unit on Applied Molecular Biosciences – UCIBIO (UIDP/04378/2020 and UIDB/04378/2020), Associate Laboratory Institute for Health and Bioeconomy - i4HB (LA/P/0140/202019), CICECO (UIDB/50011/2020, UIDP/50011/2020 & LA/P/0006/2020), LAQV/REQUIMTE (UIDB/50006/2020, UIDP/50006/2020), and iNOVA4Health (UIDB/04462/2020 and UIDP/04462/2020), through national funds from FCT - Fundação para a Ciência e a Tecnologia, I.P. and, where applicable, co-financed by the FEDER - Fundo Europeu de Desenvolvimento Regional, within the PT2020 Partnership Agreement. The Associate Laboratories LS4FUTURE (LA/P/0087/2020) are also acknowledged. Funding from INTERFACE Programme, through the Innovation, Technology and Circular Economy Fund (FITEC), is gratefully acknowledged. This work was also supported

by FCT, through the strategic project UIDB/04292/2020 awarded to MARE and through project LA/P/0069/2020 granted to the Associate Laboratory ARNET. P. C.-R. acknowledges FCT I.P. for PhD Grant SFRH/BD/131947/2017. ATS also acknowledges FCT/Ministério da Ciência, Tecnologia e Ensino Superior for the Individual Grant CEEC-IND/04801/2017.

Appendix A. Supplementary data

Supplementary data to this article can be found online at https://doi.org/10.1016/j.algal.2023.103014.

References

[1] Z. Ahmed, Y. Wang, N. Anjum, A. Ahmad, S.T. Khan, Characterization of exopolysaccharide produced by Lactobacillus kefiranofaciens ZW3 isolated from Tibet kefir – part II, Food Hydrocoll. 30 (1) (2013) 343–350, https://doi.org/10.1016/j.foodhyd.2012.06.009.

[2] S. Anastase-Ravion, M.-P. Carreno, C. Blondin, O. Ravion, J. Champion, F. Chaubet, N. Haeffner-Cavaillon, D. Letourneur, Heparin-like polymers modulate proinflammatory cytokine production by lipopolysaccharide-stimulated human monocytes, J. Biomed. Mater. Res. 60 (3) (2002) 375–383, https://doi.org/10.1002/jbm.10112.

[3] M.B. Ariede, T.M. Candido, A.L.M. Jacome, M.V.R. Velasco, J.C.M. de Carvalho, A. R. Baby, Cosmetic attributes of algae—a review, Algal Res. 25 (2017) 483–487, https://doi.org/10.1016/j.algal.2017.05.019.

[4] J. Assunção, A. Guedes, F. Malcata, Biotechnological and pharmacological applications of biotoxins and other bioactive molecules from dinoflagellates, Mar. Drugs 15 (12) (2017) 393, https://doi.org/10.3390/md15120393.

[5] S.-Y. Bae, J.H. Yim, H.K. Lee, S. Pyo, Activation of murine peritoneal macrophages by sulfated exopolysaccharide from marine microalga gyrodinium impudicum (strain KG03): involvement of the NF-κB and JNK pathway, Int. Immunopharmacol. 6 (3) (2006) 473–484.

[6] A.B. Blakeney, P.J. Harris, R.J. Henry, B.A. Stone, A simple and rapid preparation of alditol acetates for monosaccharide analysis, Carbohydr. Res. 113 (2) (1983) 291–299.

[7] N. Blumenkrantz, G. Asboe-Hansen, New method for quantitative determination of uronic acid, Anal. Biochem. 54 (1973) 484–489.

[8] W.-T. Choo, M.-L. Teoh, S.-M. Phang, P. Convey, W.-H. Yap, B.-H. Goh, J. Beardall, Microalgae as potential anti-inflammatory natural product against human inflammatory skin diseases, Front. Pharmacol. 11 (2020) 1086, https://doi.org/10.3389/fphar.2020.01086.

[9] P. Concórdio-Reis, V.D. Alves, X. Moppert, J. Guézennec, F. Freitas, M.A.M. Reis, Characterization and biotechnological potential of extracellular polysaccharides synthesized by alteromonas strains isolated from French Polynesia marine environments, Mar. Drugs 19 (9) (2021) 522, https://doi.org/10.3390/md19090522.

[10] P. Concórdio-Reis, C.V. Pereira, M.P. Batista, C. Sevrin, C. Grandfils, A.C. Marques, E. Fortunato, F.B. Gaspar, A.A. Matias, F. Freitas, M.A.M. Reis, Silver nanocomposites based on the bacterial fucose-rich polysaccharide secreted by Enterobacter A47 for wound dressing applications: synthesis, characterization and in vitro bioactivity, Int. J. Biol. Macromol. (2020), https://doi.org/10.1016/j.ijbiomac.2020.07.072.

[11] P. Concórdio-Reis, J.R. Pereira, C.A.V. Torres, C. Sevrin, C. Grandfils, F. Freitas, Effect of mono- and dipotassium phosphate concentration on extracellular polysaccharide production by the bacterium Enterobacter A47, Process Biochem. (2018), https://doi.org/10.1016/j.procbio.2018.09.001.

[12] C. Delattre, G. Pierre, C. Laroche, P. Michaud, Production, extraction and characterization of microalgal and cyanobacterial exopolysaccharides, Biotechnol. Adv. 34 (7) (2016) 1159–1179, https://doi.org/10.1016/j.biotechadv.2016.08.001.

[13] K.S. Dodgson, R.G. Price, A note on the determination of the ester sulphate content of sulphated polysaccharides, Biochem. J. 84 (1) (1962) 106.

[14] F. Dourado, P. Madureira, V. Carvalho, R. Coelho, M.A. Coimbra, M. Vilanova, M. Mota, F.M. Gama, Purification, structure and immunobiological activity of an arabinan-rich pectic polysaccharide from the cell walls of Prunus dulcis seeds, Carbohydr. Res. 339 (15) (2004) 2555–2566.

[15] S. Dutta, P. Bhadury, Effect of arsenic on exopolysaccharide production in a diazotrophic cyanobacterium, J. Appl. Phycol. 32 (5) (2020) 2915–2926, https://doi.org/10.1007/s10811-020-02206-0.

[16] I. Farinha, P. Duarte, A. Pimentel, E. Plotnikova, B. Chagas, L. Mafra, C. Grandfils, F. Freitas, E. Fortunato, M.A.M. Reis, Chitin–glucan complex production by komagataella pastoris: downstream optimization and product characterization, Carbohydr. Polym. 130 (2015) 455–464, https://doi.org/10.1016/j.carbpol.2015.05.034.

[17] A.S. Ferreira, I. Mendonça, I. Póvoa, H. Carvalho, A. Correia, M. Vilanova, T. H. Silva, M.A. Coimbra, C. Nunes, Impact of growth medium salinity on galactoxylan exopolysaccharides of Porphyridium purpureum, Algal Res. 59 (2021), 102439.

[18] S.S. Ferreira, C.P. Passos, P. Madureira, M. Vilanova, M.A. Coimbra, Structure–function relationships of immunostimulatory polysaccharides: a review, Carbohydr. Polym. 132 (2015) 378–396, https://doi.org/10.1016/j.carbpol.2015.05.079.

[19] F. Freitas, C.A.V. Torres, D. Araújo, I. Farinha, J.R. Pereira, P. Concórdio-Reis, M.A. M. Reis, Advanced microbial polysaccharides, in: B. Rehm, M.F. Moradali (Eds.), Biopolymers for Biomedical and Biotechnological Applications, 1st ed., Wiley, 2021, pp. 19–62, https://doi.org/10.1002/9783527818310.ch2.

[20] C. Gaignard, C. Laroche, G. Pierre, P. Dubessay, C. Delattre, C. Gardarin, P. Gourvil, I. Probert, A. Dubuffet, P. Michaud, Screening of marine microalgae: investigation of new exopolysaccharide producers, Algal Res. 44 (2019), 101711, https://doi.org/10.1016/j.algal.2019.101711.

[21] F. Gao, S. Woolschot, I.T.D. Cabanelas, R.H. Wijffels, M.J. Barbosa, Light spectra as triggers for sorting improved strains of Tisochrysis lutea, Bioresour. Technol. 321 (2021), 124434, https://doi.org/10.1016/j.biortech.2020.124434.

[22] S. Gedikli, G. Güngör, Y. Toptaş, D.E. Sezgin, M. Demirbilek, N. Yazıhan, P. Aytar Çelik, E.B. Denkbaş, V. Bütün, A. Çabuk, Optimization of hyaluronic acid production and its cytotoxicity and degradability characteristics, Prep. Biochem. Biotechnol. 1–9 (2018), https://doi.org/10.1080/10826068.2018.1476885.

[23] B.M. Guerreiro, F. Freitas, J.C. Lima, J.C. Silva, M. Dionísio, M.A.M. Reis, Demonstration of the cryoprotective properties of the fucose-containing polysaccharide FucoPol, Carbohydr. Polym. 245 (2020), 116500, https://doi.org/10.1016/j.carbpol.2020.116500.

[24] R.R.L. Guillard, J.H. Ryther, Studies of marine planktonic diatoms. I. Cyclotella nana Hustedt, and Detonula confervacea (cleve) Gran, Canadian Journal of Microbiology 8 (2) (1962) 229–239, https://doi.org/10.1139/m62-029.

[25] M. Hamed, E. Coelho, R. Bastos, D.V. Evtuguin, S.S. Ferreira, T. Lima, M. Vilanova, A. Sila, M.A. Coimbra, A. Bougatef, Isolation and identification of an arabinogalactan extracted from pistachio external hull: assessment of immunostimulatory activity, Food Chem. 373 (2022), 131416, https://doi.org/10.1016/j.foodchem.2021.131416.

[26] M. Hasui, M. Matsuda, K. Okutani, S. Shigeta, In vitro antiviral activities of sulfated polysaccharides from a marine microalga (Cochlodinium polykrikoides) against human immunodeficiency virus and other enveloped viruses, Int. J. Biol. Macromol. 17 (5) (1995) 293–297, https://doi.org/10.1016/0141-8130(95)98157-T.

[27] M. Hasui, M. Matsuda, S. Yoshimatsu, K. Okutani, Production of a lactate-associated galactan sulfate by a dinoflagellate gymnodinium A3, Fish. Sci. 61 (2) (1995) 321–326, https://doi.org/10.2331/fishsci.61.321.

[28] P. Jajesniak, H.E.M. Omar Ali, T.S. Wong, Carbon dioxide capture and utilization using biological systems: opportunities and challenges, J. Bioprocess. Biotechn. 04 (03) (2014), https://doi.org/10.4172/2155-9821.1000155.

[29] T.U. Jayawardena, K.K.A. Sanjeewa, D.P. Nagahawatta, H.-G. Lee, Y.-A. Lu, A.P.J. P. Vaas, D.T.U. Abeytunga, C.M. Nanayakkara, D.-S. Lee, Y.-J. Jeon, Anti-inflammatory effects of sulfated polysaccharide from Sargassum swartzii in macrophages via blocking TLR/NF-Kb signal transduction, Mar. Drugs 18 (12) (2020) 601, https://doi.org/10.3390/md18120601.

[30] M. Jesus Raposo, A. Morais, R. Morais, Marine polysaccharides from algae with potential biomedical applications, Mar. Drugs 13 (5) (2015) 2967–3028, https://doi.org/10.3390/md13052967.

[31] S.L.R.K. Kanamarlapudi, S. Muddada, Characterization of exopolysaccharide produced by Streptococcus thermophilus CC30, Biomed. Res. Int. 2017 (2017) 1–11, https://doi.org/10.1155/2017/4201809.

[32] M.-C. Kang, H. Lee, H.-D. Choi, Y.-J. Jeon, Antioxidant properties of a sulfated polysaccharide isolated from an enzymatic digest of Sargassum thunbergii, Int. J. Biol. Macromol. 132 (2019) 142–149, https://doi.org/10.1016/j.ijbiomac.2019.03.178.

[33] R.R. Klosterhoff, J.M. Bark, N.M. Glänzel, M. Iacomini, G.R. Martinez, S.M. B. Winnischofer, L.M.C. Cordeiro, Structure and intracellular antioxidant activity of pectic polysaccharide from acerola (Malpighia emarginata), Int. J. Biol. Macromol. 106 (2018) 473–480, https://doi.org/10.1016/j.ijbiomac.2017.08.032.

[34] O. Levy-Ontman, M. Huleihel, R. Hamias, T. Wolak, E. Paran, An anti-inflammatory effect of red microalga polysaccharides in coronary artery endothelial cells, Atherosclerosis 264 (2017) 11–18, https://doi.org/10.1016/j.atherosclerosis.2017.07.017.

[35] L. Liu, G. Pohnert, D. Wei, Extracellular metabolites from industrial microalgae and their biotechnological potential, Mar. Drugs 14 (10) (2016) 191, https://doi.org/10.3390/md14100191.

[36] H. Maalej, D. Moalla, C. Boisset, S. Bardaa, H.B. Ayed, Z. Sahnoun, T. Rebai, M. Nasri, N. Hmidet, Rhelogical, dermal wound healing and in vitro antioxidant properties of exopolysaccharide hydrogel from Pseudomonas stutzeri AS22, Colloids Surf. B: Biointerfaces 123 (2014) 814–824, https://doi.org/10.1016/j.colsurfb.2014.10.017.

[37] S.K. Mandal, R.P. Singh, V. Patel, Isolation and characterization of exopolysaccharide secreted by a toxic dinoflagellate, Amphidinium carterae hulburt 1957 and its probable role in harmful algal blooms (HABs), Microb. Ecol. 62 (3) (2011) 518–527, https://doi.org/10.1007/s00248-011-9852-5.

[38] M.S. Matos, R. Romero-Díez, A. Álvarez, M.R. Bronze, S. Rodríguez-Rojo, R. B. Mato, M.J. Cocero, A.A. Matias, Polyphenol-rich extracts obtained from winemaking waste streams as natural ingredients with cosmeceutical potential, Antioxidants 8 (9) (2019) 355, https://doi.org/10.3390/antiox8090355.

[39] E.V. Medina-Cabrera, B. Rühmann, J. Schmid, V. Sieber, Characterization and comparison of Porphyridium sordidum and Porphyridium purpureum concerning growth characteristics and polysaccharide production, Algal Res. 49 (2020), 101931, https://doi.org/10.1016/j.algal.2020.101931.

[40] A. Olafsdottir, G.E. Thorlacius, S. Omarsdottir, E.S. Olafsdottir, A. Vikingsson, J. Freysdottir, I. Hardardottir, A heteroglycan from the cyanobacterium Nostoc commune modulates LPS-induced inflammatory cytokine secretion by THP-1

monocytes through phosphorylation of ERK1/2 and akt, Phytomedicine 21 (11) (2014) 1451–1457, https://doi.org/10.1016/j.phymed.2014.04.023.
[41] C. Pagano, D. Puglia, F. Luzi, A.D. Michele, S. Scuota, S. Primavilla, M.R. Ceccarini, T. Beccari, C.A.V. Iborra, D. Ramella, M. Ricci, L. Perioli, Development and characterization of xanthan gum and alginate based bioadhesive film for pycnogenol topical use in wound treatment, Pharmaceutics 13 (3) (2021) 324, https://doi.org/10.3390/pharmaceutics13030324.
[42] C.O. Pandeirada, É. Maricato, S.S. Ferreira, V.G. Correia, B.A. Pinheiro, D. V. Evtuguin, A.S. Palma, A. Correia, M. Vilanova, M.A. Coimbra, C. Nunes, Structural analysis and potential immunostimulatory activity of nannochloropsis oculata polysaccharides, Carbohydr. Polym. 222 (2019), 114962, https://doi.org/10.1016/j.carbpol.2019.06.001.
[43] A. Parikh, D. Madamwar, Partial characterization of extracellular polysaccharides from cyanobacteria, Bioresour. Technol. 97 (15) (2006) 1822–1827, https://doi.org/10.1016/j.biortech.2005.09.008.
[44] C.P. Passos, M.A. Coimbra, Microwave superheated water extraction of polysaccharides from spent coffee grounds, Carbohydr. Polym. 94 (1) (2013) 626–633.
[45] R. Paz-Samaniego, E. Carvajal-Millan, F. Brown-Bojorquez, A. Rascón-Chu, Y. L. López-Franco, N. Sotelo-Cruz, J. Lizardi-Mendoza, Gelation of arabinoxylans from maize wastewater—effect of alkaline hydrolysis conditions on the gel rheology and microstructure, in: M. Samer (Ed.), Wastewater Treatment Engineering, InTech, 2015, https://doi.org/10.5772/61022.
[46] F.A. Pettolino, C. Walsh, G.B. Fincher, A. Bacic, Determining the polysaccharide composition of plant cell walls, Nat. Protoc. 7 (9) (2012) 1590–1607.
[47] P. Roux, R. Siano, K. Collin, G. Bilien, C. Sinquin, L. Marchand, A. Zykwinska, C. Delbarre-Ladrat, M. Schapira, Bacteria enhance the production of extracellular polymeric substances by the green dinoflagellate lepidodinium chlorophorum, Sci. Rep. 11 (1) (2021) 4795, https://doi.org/10.1038/s41598-021-84253-2.
[48] S. Roy Chowdhury, S. Sengupta, S. Biswas, T.K. Sinha, R. Sen, R.K. Basak, B. Adhikari, A. Bhattacharyya, Bacterial fucose-rich polysaccharide stabilizes MAPK-mediated Nrf2/Keap1 signaling by directly scavenging reactive oxygen species during hydrogen peroxide-induced apoptosis of human lung fibroblast cells, PLoS ONE 9 (11) (2014), e113663, https://doi.org/10.1371/journal.pone.0113663.
[49] R.R. Selvendran, J.F. March, S.G. Ring, Determination of aldoses and uronic acid content of vegetable fiber, Anal. Biochem. 96 (2) (1979) 282–292.
[50] A.T. Serra, A.A. Matias, R.F.M. Frade, R.O. Duarte, R.P. Feliciano, M.R. Bronze, M. E. Figueira, A. de Carvalho, C.M.M. Duarte, Characterization of traditional and exotic apple varieties from Portugal. Part 2 – antioxidant and antiproliferative activities, J. Funct. Foods 2 (1) (2010) 46–53, https://doi.org/10.1016/j.jff.2009.12.005.
[51] L. Shao, Z. Wu, H. Zhang, W. Chen, L. Ai, B. Guo, Partial characterization and immunostimulatory activity of exopolysaccharides from lactobacillus rhamnosus KF5, Carbohydr. Polym. 107 (2014) 51–56, https://doi.org/10.1016/j.carbpol.2014.02.037.
[52] S. Singh, C. Kant, R.K. Yadav, Y.P. Reddy, G. Abraham, Cyanobacterial exopolysaccharides: composition, biosynthesis, and biotechnological applications, in: Cyanobacteria, Elsevier, 2019, pp. 347–358, https://doi.org/10.1016/B978-0-12-814667-5.00017-9.
[53] Z.-J. Su, Y.-Y. Wei, D. Yin, X.-H. Shuai, Y. Zeng, T.-J. Hu, Effect of sophora subprosrate polysaccharide on oxidative stress induced by PCV2 infection in RAW264.7 cells, Int. J. Biol. Macromol. 62 (2013) 457–464, https://doi.org/10.1016/j.ijbiomac.2013.09.026.
[54] I. Uhliariková, M. Matulová, P. Capek, Optimizing acid hydrolysis for monosaccharide compositional analysis of Nostoc cf. Linckia acidic exopolysaccharide, Carbohydr. Res. 508 (2021), 108400, https://doi.org/10.1016/j.carres.2021.108400.
[55] K. Umemura, K. Yanase, M. Suzuki, K. Okutani, T. Yamori, T. Andoh, Inhibition of DNA topoisomerases I and II, and growth inhibition of human cancer cell lines by a marine microalgal polysaccharide, Biochem. Pharmacol. 66 (3) (2003) 481–487, https://doi.org/10.1016/S0006-2952(03)00281-8.
[56] H.-M.D. Wang, X.-C. Li, D.-J. Lee, J.-S. Chang, Potential biomedical applications of marine algae, Bioresour. Technol. 244 (2017) 1407–1415, https://doi.org/10.1016/j.biortech.2017.05.198.
[57] R. Xiao, Y. Zheng, Overview of microalgal extracellular polymeric substances (EPS) and their applications, Biotechnol. Adv. 34 (7) (2016) 1225–1244, https://doi.org/10.1016/j.biotechadv.2016.08.004.
[58] L. Xie, M. Shen, P. Wen, Y. Hong, X. Liu, J. Xie, Preparation, characterization, antioxidant activity and protective effect against cellular oxidative stress of phosphorylated polysaccharide from cyclocarya paliurus, Food Chem. Toxicol. 145 (2020), 111754, https://doi.org/10.1016/j.fct.2020.111754.
[59] J.H. Yim, S.J. Kim, S.H. Ahn, C.K. Lee, K.T. Rhie, H.K. Lee, Antiviral effects of sulfated exopolysaccharide from the marine microalga gyrodinium impudicum strain KG03, Mar. Biotechnol. 6 (1) (2004) 17–25, https://doi.org/10.1007/s10126-003-0002-z.
[60] J.H. Yim, S.J. Kim, S.H. Ahn, H.K. Lee, Optimal conditions for the production of sulfated polysaccharide by marine microalga gyrodinium impudicum strain KG03, Biomol. Eng. 20 (4–6) (2003) 273–280, https://doi.org/10.1016/S1389-0344(03)00070-4.
[61] J.H. Yim, S.J. Kim, S.H. Ahn, H.K. Lee, Characterization of a novel bioflocculant, p-KG03, from a marine dinoflagellate, gyrodinium impudicum KG03, Bioresour. Technol. 98 (2) (2007) 361–367, https://doi.org/10.1016/j.biortech.2005.12.021.